International Immunology, Vol. 28, No. 10, pp. 503–512
doi:10.1093/intimm/dxw031
Advance Access publication 28 June 2016

Inflammatory responses increase secretion of MD-1 protein

Richard Thomas Jennings[1], Erdenezaya Odkhuu[2], Akina Nakashima[2], Naoko Morita[2], Toshihiko Kobayashi[3], Ikuko Yamai[1], Miyako Tanaka[4], Takayoshi Suganami[4], Sanae Haga[5], Michitaka Ozaki[5], Yasuharu Watanabe[6], Yoshinori Nagai[6,7], Kiyoshi Takatsu[6,8], Takane Kikuchi-Ueda[9], Isao Ichimonji[2], Yoshihiro Ogawa[10,11], Hidekazu Takagi[2], Tatsuya Yamazaki[2], Kensuke Miyake[1] and **Sachiko Akashi-Takamura[2]**

[1]Division of Innate Immunity, Department of Microbiology and Immunology, Institute of Medical Science, University of Tokyo, 4-6-1, Shirokanedai, Minato-ku, Tokyo 108-8639, Japan
[2]Department of Microbiology and Immunology, School of Medicine, Aichi Medical University, 1-1, Yazakokarimata, Nagakute, Aichi 480-1195, Japan
[3]Department of Molecular Immunology and Inflammation, Research Institute, National Center for Global Health and Medicine, 1-21-1, Toyama, Shinjyuku-ku, Tokyo 162-8655, Japan
[4]Department of Molecular Medicine and Metabolism, Research Institute of Environmental Medicine, Nagoya University, Furo-cho, Chikusa-ku, Nagoya 464-8601, Japan
[5]Laboratory of Molecular and Functional Bio-imaging, Faculty of Health Sciences, Hokkaido University, Kita-ku, Sapporo, Hokkaido 060-0812, Japan
[6]Department of Immunobiology and Pharmacological Genetics, Graduate School of Medicine and Pharmaceutical Science for Research, University of Toyama, 2630, Toyama 930-0194, Japan
[7]JST, PRESTO, 4-1-8, Kawaguchi, Saitama 332-0012, Japan
[8]Toyama Prefectural Institute for Pharmaceutical Research, 17-1, Irimizu, Toyama 939-0363, Japan
[9]Department of Microbiology and Immunology, School of Medicine, Teikyo University, 2-11-1, Itabashi-ku, Tokyo 173-8605, Japan
[10]Department of Molecular Endocrinology and Metabolism, Graduate School of Medical and Dental Sciences, Tokyo Medical and Dental University, 1-5-45, Bunkyo-ku, Tokyo 113-8510, Japan
[11]AMED, CREST, 1-7-1, Chiyoda-ku, Tokyo 100-0004, Japan

Corresponding to: S. Akashi-Takamura; E-mail: sachiko@aichi-med-u.ac.jp

Received 10 August 2015, *accepted* 21 June 2016

Abstract

Radioprotective 105 (RP105) is a type I transmembrane protein, which associates with a glycoprotein, MD-1. Monoclonal antibody (mAb)-mediated ligation of RP105/MD-1 robustly activates B cells. RP105/MD-1 is structurally similar to Toll-like receptor 4 (TLR4)/MD-2. B-cell responses to TLR2 and TLR4/MD-2 ligands are impaired in the absence of RP105 or MD-1. In addition to RP105/MD-1, MD-1 alone is secreted. The structure of MD-1 shows that MD-1 has a hydrophobic cavity that directly binds to phospholipids. Little is known, however, about a ligand for MD-1 and the role of MD-1 *in vivo*. To study the role of RP105/MD-1 and MD-1 alone, specific mAbs against MD-1 are needed. Here, we report the establishment and characterization of two anti-MD-1 mAbs (JR2G9, JR7G1). JR2G9 detects soluble MD-1, whereas JR7G1 binds both soluble MD-1 and the cell surface RP105/MD-1 complex. With these mAbs, soluble MD-1 was detected in the serum and urine. The MD-1 concentration was altered by infection, diet and reperfusion injury. Serum MD-1 was rapidly elevated by TLR ligand injection in mice. The quantitative PCR and supernatant-precipitated data indicate that macrophages are one of the sources of serum soluble MD-1. These results suggest that soluble MD-1 is a valuable biomarker for inflammatory diseases.

Keywords: MD-1, monoclonal antibody, RP105

Introduction

Toll-like receptors (TLRs) are not only indispensable sensors as a protective mechanism against infection but also regulators for disease development (1). MD-1 is a soluble protein, which is associated with radioprotective 105

(RP105), also known as CD180, on B cells (2, 3). RP105 forms a complex with MD-1 and can transmit a survival and strong proliferation signal into B cells; this is known to occur upon the ligation with anti-RP105 monoclonal antibody (mAb) (4, 5). However, we have not yet known the presence of a ligand to RP105/MD-1 *in vivo*.

Mouse B cells express TLR2 and TLR4/MD-2, both of which sense microbial membrane components and non-microbial products derived from damaged tissue (6). RP105/MD-1 is structurally and functionally related to the lipopolysaccharide (LPS) sensor TLR4/MD-2 (7, 8). RP105/MD-1 is reported to be associated with TLR4/MD-2 (9), suggesting that RP105/MD-1 forms a co-cluster with TLR4/MD-2 and is activated simultaneously. Previous reports show that RP105/MD-1 works in concert with TLR2 and TLR4/MD-2 in tonic B-cell activation in the steady state (10) and had a pathogenic role in autoimmune disease in MRL/$^{lpr/lpr}$ mice (11). Furthermore, a soluble form of MD-2 protein is present in the plasma of septic patients and can opsonize gram-negative bacteria in cooperation with TLR4 (12). Recently, a soluble form of MD-1 protein in serum has also been shown. Sasaki *et al*. show that serum soluble MD-1 (sMD-1) levels increase with disease progression in autoimmune prone MRL$^{lpr/lpr}$ mice by using a flow cytometry-based assay (13). They also show that sMD-1 is constitutively secreted by bone marrow-derived macrophages (BMDM) from C57BL/6 mice. Recent structural analyses show that both MD-1 and MD-2 have lipid-binding pockets (14), which bind to phospholipids and LPS, respectively. Koarada *et al*. show that the quantity of B cells lacking cell-surface RP105 is increased in autoimmune patients, and the ratio of RP105 non-expressers to expressers correlates with the disease activity of patients (15, 16). Taken together, it seems likely that MD-1 either alone or in complex with RP105 has a role in autoimmune diseases.

We herein demonstrate the successful establishment and characterization of mAbs that recognize soluble MD-1. These mAbs were selected from hybridoma clones obtained from mouse myeloma cells fused with the spleen cells from MD-1-deficient mice immunized with MD-1-expressing cells. We established an MD-1 ELISA system using these mAbs. These data clearly show that JR2G9 and JR7G1 are useful tools for detection of serum or urine MD-1 and analysis of MD-1 biological function.

Methods

Generation of anti-mouse MD-1 mAb

To establish the anti-mouse MD-1 mAb, 16- to 20-week-old BALB/c MD-1$^{-/-}$ female mice were immunized three times with Ba/F3 cells expressing myc-tagged MD-1 transmembrane (Ba/F3-MD-1mycTM). Three days after the final immunization, collected spleen cells were fused with SP2/O myeloma cells. Hybridoma were selected based on their secretion of mAbs. The selection was verified by flow cytometry using Ba/F3-MD-1mycTM, enabling cell-surface expression of MD-1, and an immune resource from mice. These mAbs, named JR2G9 (mouse IgG1/κ) and JR7G1 (mouse IgG1/κ), were used in this study.

Mice

BALB/c mice and C57BL/6 mice were purchased from Japan SLC, Inc. (Shizuoka, Japan). All animal experiments were conducted with the approval of the Animal Research Committee of the Institute of Medical Science, the University of Tokyo, Aichi Medical University, Hokkaido University, Toyama University, and Tokyo Medical and Dental University.

MD-1 transgenic mice

The pCAGGS vector encoding the MD-1 cDNA was used for injection to fertilized eggs of mice (Unitech, Chiba, Japan). After birth, the protein level of MD-1 was checked and provided by Y.N.

High-fat high-sucrose food, culture method and period

C57BL/6 male mice were maintained in a temperature-, humidity- and light-controlled room (12-h light/dark cycles), allowed free access to water and standard chow (CE-2; 343.1 kcal per 100 g, 12.6% energy as fat; CLEA Japan, Tokyo, Japan). Eight-week-old animals were fed either a standard diet (CE-2) or HiFat/HiSucrose diet (D12079B; 468 kcal/100 g, 41% energy as fat, 34.0% sucrose, 0.21% cholesterol; Research Diets, New Brunswick, NJ, USA) for 14 weeks.

Reagents

Titer MAX gold (initial adjuvant) was purchased from Funakoshi Co., Ltd (Tokyo, Japan). Biotinylated anti-Myc mAb (9E10) was purchased from Santa Cruz. B220-Fluoresceinisothiocyanate (FITC) mAb (RA3-6B2) was purchased from eBioscience (San Diego, CA). CD11b-PE and CD11b-Phycoerythrin (PE) were purchased from Biolegend (San Diego, CA). Streptavidin-alkaline phosphatase conjugate (APC) was purchased from eBioscience or Pharmingen (San Diego, CA, USA). Lipid A purified from *Salmonella minnesota* (Re-595) and LPS from *Escherichia coli* (O55:B5) were purchased from Sigma–Aldrich. (St Louis, MO, USA). *N*-palmitoyl-S-(2,3-bis(palmitoyloxy)-(2R,S)-propyl)-(R)-cysterinyl-seryl-(lysyl)3-lysine (P3CSK4) was purchased from EMC Microcollections (Tubingen, Germany). CpG (CpG1668: TCCATGACGTTCCTGATGCT) was purchased from Hokkaido System Science (Sapporo, Japan). Goat anti-mouse IgM F (ab′)2 was purchased from Jackson Immuno Research (West Grove, PA, USA). Rat anti-mouse CD40 mAb (LB429S), rat anti-mouse RP105 mAb (RP/14) and rat anti-mouse MD-1 mAb (MD14) were purified and dialyzed with PBS. Polyclonal antibodies (pAbs) to mouse MD-1 or mouse RP105 were established in Tokyo University by immunizing each rabbit with the mouse MD-1 peptide of (DPLQDFGLSIDQCSKQ) or RP105 peptide of (CKYFLRWKYQHI).

Cells

The interleukin-3 (IL-3)-dependent line Ba/F3 was transfected with the pEFBOS expression vector encoding a mouse RP105 and mouse MD-1. Ba/F3 expressing RP105/MD-1 was established as described previously (17, 18). The encoding of mouse MD-1 of pEFBOS expression vector and transmembrane portion of pDisplay vetor (Invitrogen,

Carlsbad, CA, USA) were cloned into the pMXp retrovial vector (MD-1mycTM vector). Ba/F3 was transducted with the pMXp MD-1 mycTM vector by virus supernatant of PLAT-E cells. The cells expressing MD-1 myc fused with a transmembrane domain enabled cell-surface expression (Ba/MD-1mycTM). BMDM or bone marrow-derived dendritic cells (BMDC) were prepared from 16- to 20-week C57BL/6 female mice. Bone marrow cells were placed in 10-cm dishes with 10% FCS-DMEM supplemented with 100 ng/ml recombinant murine M-CSF (peprotech). At day 6, adherent cells were harvested and used as BMDM. Bone marrow cells were placed at 1×10^6 cells/ml in 24-well plates with 10% FCS-RPMI 1640 supplemented with 10 ng/ml recombinant murine GM-CSF (peprotech). On day 6, loosely adherent cells were collected and used as BMDC.

Immunoprecipitation

Cells were lysed on ice for 15 min with lysis buffer containing 150 mM NaCl, 50 mM Tris–HCl (pH 7.4), 5 mM EDTA, aprotinin (10 μg/ml), leupeptin (10 μg/ml), 1 mM phenylmethylsulfonyl fluoride and 1% Triton X-100. Lysates were separated from debris by centrifugation at 13 000 r.p.m. at 4°C for 15 min and then incubated with antibody-conjugated beads at 4°C for 2 h. Beads were washed three times and boiled at 95°C for 5 min in the sample buffer for SDS–PAGE. Bound proteins were subjected to SDS–PAGE and western blot analysis. Reagents used for immune-probing were anti-RP105 pAb, anti-MD-1 pAb and anti-biotinylated Myc mAb. The second antibodies were goat anti-rabbit IgG-APC (Bio-Rad Laboratories, Hercules, CA, USA) or streptavidin-APC (Calbiochem, San Diego, CA, USA). In the serum immunoprecipitation (IP) assay, collected serum was diluted five times with Tris/saline buffer [50 mM Tris–HCl (pH 7.4), 150 mM NaCl, 0.1% sodium azide], then incubated with antibody-conjugated beads at 4°C for 2 h. After IP, we performed the experiments in the same way as above.

Endo H and N-glycosidase assay

Serum immunoprecipitated samples were eluted with sample buffer (70 mM Tris, 1% SDS, 10% glycerol, 0.005% bromophenol blue, pH 6.8) and treated with endo H or *N*-glycosidase according to the manufacturer's instructions (New England Biolabs, Inc.). Samples were subjected to SDS–PAGE and immunoprobing in a way same as the above-mentioned IP method. Immunoreactive bands were visualized using the enhanced chemiluminescence ECL substrate (GE Healthcare) and a LAS4000 imaging system (GE Healthcare).

Immunofluoresence staining

Cells were incubated for 15 min at 4°C with the primary biotinylated mAbs diluted in staining buffer (PBS containing 2.5% FBS and 0.01% NaN_3). Cells were washed with staining buffer and incubated with APC-conjugated streptavidin (Biolegend, San Diego, CA, USA) and B220-FITC, or CD11b-PE, or CD11c-PE for 15 min at 4°C. Flow cytometry analysis was performed on a FACS Calibur system or FACS Canto (BD, Franklin Lakes, NJ, USA).

Protection from cell death by dexamethasone

For experiments on dexamethasone-induced apoptosis, spleen cells were placed in a 96-well plate (2×10^5/well) and preincubated with antibodies (10 μg/ml) for 2 h. Then, several concentrations of dexamethasone (Sigma–Aldrich, San Diego, CA, USA) were added to cultures simultaneously with antibodies and cells were cultured for 20 h. After this incubation, cells were collected and stained with propidium iodide (Biovision, Milpitas, CA, USA) and B220-FITC. In this experiment, B220-positive gated viable B cells were determined by a formula. We calculated each B-cell survival rate where 100 was the percentage that survived in the well without the antibody. The results were represented as mean ± SD for triplicate culture.

Thymidine uptake

Spleen cells were obtained from mice and prepared to single-cell suspension. After RBC lysis with Tris/NH_4Cl treatment, cells were incubated at 1×10^5/well in 96-well, flat-bottomed plates with or without TLR ligands or mAbs for 3 days. After 3-day culture, spleen cells were pulsed with [^{3}H] thymidine (PerkinElmer) for 6 h before harvesting on glass filters by using a cell harvester (Inotech, Brandon, FL, USA). Incorporation of [^{3}H] thymidine was measured by a scintillation counter (TriLux, Waltham, MA, USA).

Measurement of serum and urine MD-1 concentration

The levels of serum MD-1 were measured by ELISA. Purified JR7G1 mAb (5 μg/ml) was coated onto the ELISA plate and blocked with 1% BSA, and 10% diluted sera were applied. Bound-MD-1 was detected with biotinylated JR2G9 (1 μg/ml) and streptavidin-horseradish peroxidase (GE healthcare, Fairfield, CT, USA). Recombinant MD-1 (R&D, Minneapolis, MN, USA) was used for standard. Blood sugar and urine creatinine concentration were measured in the Nagahama LSL Company (Nagahama, Japan).

Quantitative real-time reverse transcriptase-polymerase chain reaction

The total RNAs from cells were purified with RNeasy mini kits (QIAGEN, Valencia, CA, USA). The cDNAs were then synthesized with ReverTra Ace (Toyobo, Tokyo, Japan) following the manufacturer's instructions. Quantitative real-time PCR was performed by using a PCR system (7300 Fast Real-Time PCR System, Applied Biosystems) with gene expression assays (Taqman; Applied Biosystems) for mouse MD-1 (Ly86, Mm00440240). Each sample was normalized using TaqMan gene expression assays for mouse β-actin (Mm00607939).

Surgical procedures of renal ischemia/reperfusion

Eight-week-old male C57BL/6 mice (CLEA Japan, Tokyo, Japan) were anesthetized and placed on a heating pad. Kidneys were exposed through an abdominal section, and the right kidney was removed and the vascular pedicle of the left kidney was clamped by a microaneurysm clip for 30 min after right nephrectomy (19).

Surgical procedures of hepatic ischemia/reperfusion

For the liver ischemia/reperfusion (I/R) surgery, 12-week of C57BL/6 male mice were anesthetized and heparin sulfate (100 U/kg body weight) was intravenously injected. After laparotomy, all vessels (hepatic artery, portal vein and bile duct) to the left and median liver lobes were clamped, according to a previously described method (20, 21). After 30–90 min of liver partial ischemia, these vessels were unclamped, and the hepatic circulation was restored for the specified reperfusion period. Sham-operated control mice were subjected to a laparotomy and closure without ischemia. After the 6- or 24-h reperfusions, blood samples were collected.

Statistical analysis

Data from triplicate samples and paired data were used for statistical analysis. Statistical significance was calculated by the Student's *t*-test. A value of $P < 0.05$ was considered statistically significant. Similar results were obtained in three independent experiments.

Results

Generation of mAbs against MD-1

To generate mAbs, we established Ba/F3 cells expressing myc-MD-1 on the cell surface (Ba/MD-1mycTM). The expression level is shown by FACS analysis with anti-myc staining (Fig. 1A). MD-1$^{-/-}$BALB/c mice were immunized with the Ba/MD-1mycTM cells. Splenic cells from the immunized mice were fused with SP2/0 myeloma cells, and positive clones were screened by cell-surface staining of Ba/MD-1mycTM, which were used for immunization. We established two clones of anti-MD-1 mAb (JR7G1 and JR2G9). MD14, which was reported as an anti-mouse MD-1 mAb (3), was only able to detect the RP105-associated MD-1. Whereas, JR2G9 is able to recognize the MD-1 alone, and JR7G1 is able to recognize both MD-1 alone and MD-1 when in complex with RP105 (Fig. 1A).

Characterization of anti-MD-1 mAbs

To investigate whether the established antibodies were able to detect endogenous MD-1, we stained splenic cells from C57BL/6 wild type, RP105$^{-/-}$, or MD-1$^{-/-}$ mice. Unlike JR2G9, MD14 and JR7G1 were able to detect the MD-1 in complex with RP105 on B220-gated spleen B cells from B6 wild-type mice (Fig. 1B). Neither MD14 nor JR7G1 were able to recognize any cell-surface MD-1 on B lymphocyte harvested from RP105$^{-/-}$ mice. We also stained BMDC and BMDM with these anti-MD-1 mAbs, and similar results were obtained (Supplementary Fig. S1A and B, available at *International Immunology* Online). These results show that RP105 is required for the cell surface anchoring of MD-1 on the B cells, BMDC and BMDM.

Epitope analysis of mAbs

We examined whether these mAbs were able to precipitate MD-1 by immunoprecipitation (IP) assay. Ba/F3 cells expressing RP105/MD-1 were examined by IP with anti-MD-1 mAbs and detected by anti-RP105 pAb or anti-MD-1 pAb.

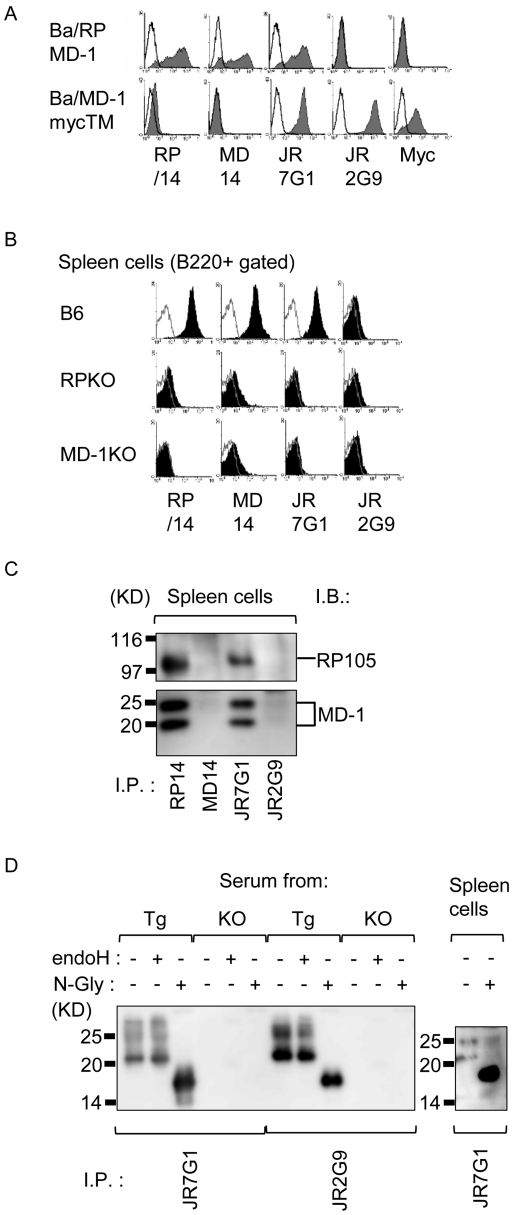

Fig. 1. Specificity of new anti-MD-1 mAbs. (A) Ba/F3 cell lines expressing RP105/MD-1 (Ba/RPMD-1) or MD-1 myc transmembrane (Ba/MD-1mycTM) were stained with indicated biotinylated mAbs, followed by streptavidin-PE as a secondary antibody. The open histogram represents staining with streptavidin-PE alone. (B) Spleen cells from 12-week B6 wild-type, B6RP105$^{-/-}$ or B6MD-1$^{-/-}$ female mice were stained with indicated biotinylated mAb, followed by streptavidin-PE. B220-positive gated B cells data are shown. (C) The cell lysate of spleen cells from B6 wild-type mice was immunoprecipitated with indicated mAbs. Precipitates were probed with anti-RP105 or anti-MD-1 polyclonal Abs, followed by biotinylated goat anti-rabbit Ig as a secondary antibody, finally followed by streptavidin-horseradish peroxidase (HRP) conjugated antibody. (D) The serum from 16 weeks B6/MD-1 transgenic mice or MD-1$^{-/-}$ female mice was immune precipitated with anti-MD-1 mAbs (JR7G1, JR2G9). Precipitated samples were treated with or without endo H, or *N*-glycosidase, as indicated in the figure. Precipitates were probed with anti-MD-1 polyclonal Ab, followed by biotinylated goat anti-rabbit Ig as a secondary antibody, finally followed by streptavidin-HRP conjugated antibody. Similar results were obtained in three independent experiments.

In the JR2G9-precipitated samples, only a small amount of MD-1 was precipitated, and association with RP105 was not found (Supplementary Fig. S1C, available at *International Immunology* Online). In the IP sample of Ba/F3 cells expressing MD-1-myc TM, MD-1-myc was clearly precipitated even in the JR2G9-precipitated sample. These results are compatible with FACS data (Fig. 1A). These results show that the recognition epitope of JR2G9 is different from JR7G1. It is considered that the MD-1epitope of JR2G9 seems close to the RP105-binding site because JR2G9 is not able to bind the RP105-expressed cells.

We also examined the antibodies' ability to precipitate endogenous MD-1 of mouse origin (Fig. 1C; Supplementary Fig. S1C, available at *International Immunology* Online). MD-1 in the spleen cell lysate was clearly detected as two bands (20 kD, 22 kD) by JR7G1 IP, but it was barely detected by JR2G9. This is consistent with the data in Fig. 1A. We also checked the existence of serum MD-1 by IP assay (Fig. 1D). Both JR mAbs precipitated the two bands, but one of the two was slightly higher (32 kD) than that detected from cell lysates (32 kD instead of 22 kD). These bands corresponded to MD-1 because they were detected with anti-MD-1 pAb; furthermore, they were not detected in serum IP samples derived from MD-1 knockout mice. Since we suspected the reason of the different molecular weights between serum and spleen might be a difference of glycosylation, we treated the anti-MD-1 mAb-immunoprecipitated samples with the endoglycosidase H (endo H) or *N*-glycanase (*N*-Gly), and conducted western analysis by using anti-MD-1 pAb. As shown in Fig. 1D, both serum and spleen MD-1 are resistant to endo H but sensitive to *N*-Gly treatment and finally both MD-1 forms are cleaved to a 17 kD molecular weight. These data demonstrate that the difference of MD-1 molecular weight between serum and spleen depends on the glycosylation. These results confirm that the newly established mAbs can efficiently detect MD-1 by both flow cytometry and immunoprecipitation assay.

Functional assay of mAbs

Anti-RP105 mAb induces antiapoptotic signaling through RP105/MD-1 and rescues spleen cells from dexamethasone-induced apoptosis (22). To further discern this antiapoptotic effect, we studied the effects of anti-MD-1 mAb in dexamethasone-induced apoptosis (Fig. 2A). An average of the survival rate in a culture medium only is set to 100%. According to the former articles, RP/14 incubation increases the survival rate from 100 to 109.5%. In the 5 or 50 nM dexamethasone-incubated wells, preincubation of RP/14 increased the survival ratio in comparison with medium only incubated wells from 28.6 to 86.5% (5 nM) and from 12.0 to 77.7% (50 nM). Preincubation of JR7G1 slightly increased the survival ratio from 28.6 to 46.5% (5 nM) and from 12.0 to 23.3% (50 nM). Although being weaker than RP/14, JR7G1 can improve the spleen cell survival from dexamethasone-induced cell death.

To analyze whether anti-MD-1 also induces proliferation of spleen cells, spleen cells were incubated with established mAbs, then proliferation was analyzed by ^{3}H-uptake (Fig. 2B, white bar). The spleen cell number increased in JR7G1 treated wells. This means that JR7G1 is an agonistic antibody. Co-stimulation with mAb and TLR ligands (Lipid A,

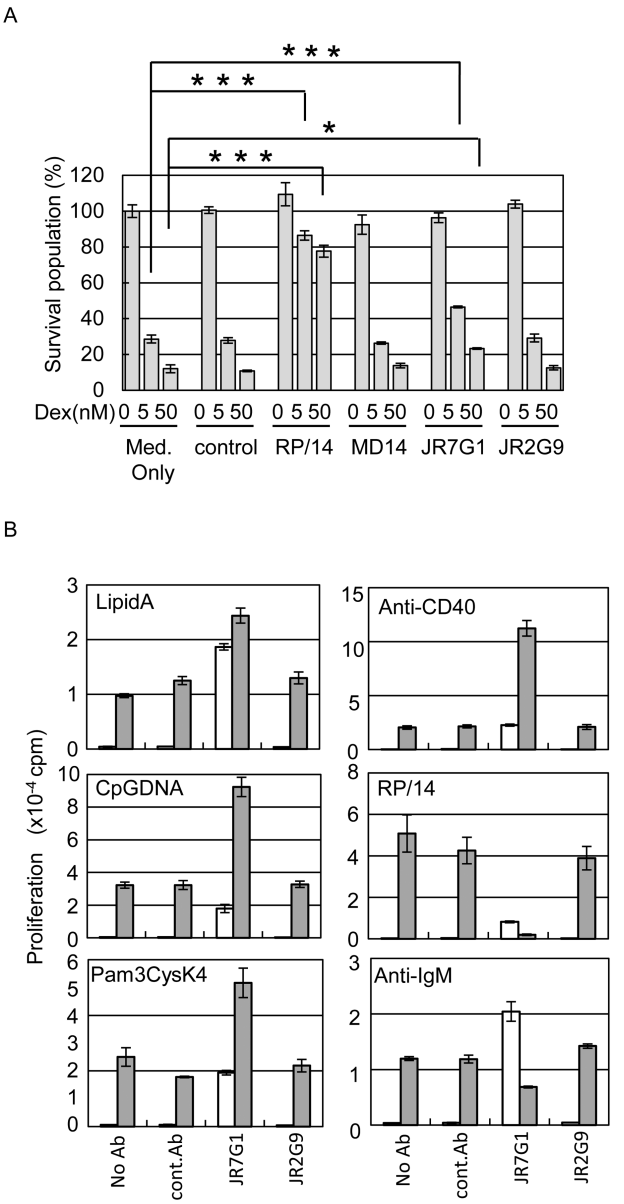

Fig. 2. Functional analysis of anti-MD-1 mAbs. (A) Spleen cells from 12-week B6 female mice were cultured for 20 h with or without dexamethasone at concentrations indicated in the figure. Indicated mAbs were present during culture at a concentration of 10 μg/ml. After incubation, cells were collected and stained with B220-FITC and propidium iodide (PI). B220-positive and PI-negative cells were regarded as survival B cells. The survival population average of wells incubated in medium only was regarded as 100%. Similar results were obtained in three independent experiments. (B) Spleen cells prepared from 12-week B6 female mice were incubated with or without mAbs indicated at the bottom [JR7G1 (10 mg/ml), JR2G9 (10 mg/ml) or control mAb (10 mg/ml)] (in white bar graph). In addition to the above-mentioned antibody, the stimulant [Lipid A (100 ng/ml), CpGDNA (1 mM), Pam3CysK4 (100 ng/ml)] or B-cell-activated mAb [anti-CD40 (1 mg/ml), anti-RP105 (1 mg/ml), anti-IgM (1 mg/ml)] (in gray bar graph) indicated at the top was added more at that same time. They were incubated for 3 days. Results are shown as mean values of counts per minute from triplicate wells with standard deviation. $^{*}P < 0.05$, $^{***}P < 0.005$. Similar results were obtained in three independent experiments.

CpGDNA and Pam3CysK4) led to a synergistic increase in proliferation (Fig. 2B, left side, gray bars). JR7G1 also augments anti-CD40 mAb-induced proliferation similarly to augmenting TLR stimulation. These results show that JR7G1 is a weak agonistic antibody. On the other hand, JR7G1 completely inhibited the RP/14 or partially inhibited the anti-IgM induced proliferation (Fig. 2B, right lower two graphs). It is suggested that not only anti-RP105 mAb but also anti-MD-1 mAb is able to induce an aggregation of RP105/MD-1 complex. These results show that MD-1 is important for the survival of spleen cells in dexamethasone-induced apoptosis and TLR ligand-induced proliferation.

Establishment of MD-1 ELISA system

IP assay with anti-MD-1 mAbs clearly shows the existence of MD-1 in serum (Fig. 1D). To quantitatively determine the concentration, we established the MD-1 ELISA system. We found the using JR7G1 (as a catching antibody) and JR2G9 (as a detecting antibody) had a higher sensitivity than any other combination of commercially available anti-MD-1 antibodies. By using these antibodies, we found that the serum MD-1 concentration of B6 wild-type mice is 0.29–0.91 μg/ml in the steady state (Supplementary Fig. S2, available at *International Immunology* Online). MD-1 also exists in the serum of RP105$^{-/-}$ mice, but the concentration is slightly higher than observed in serum of B6 mice. There is a tendency that MD-1 serum concentration increases slightly with age (Supplementary Fig. S2, available at *International Immunology* Online).

MD-1 associates with RP105 and sensitizes both TLR2 and TLR4 responses. These TLRs rapidly sense bacterial structures on the cell surface and induce immunological reaction during host defense against bacteria. To analyze MD-1 concentration during infection, we injected mice with TLR ligands (LPS, Pam3CysK4 and DH5α) and collected the serum at the indicated times (Fig. 3A). We found that the concentration of MD-1 in the serum increased according with time after injection (Fig. 3A). We also analyzed the serum cytokine production after injection of DH5α (Fig. 3B). Unlike TNF-α, the production of IL-6, IL-12p40 and CCL5 increased with time. These results suggest that MD-1 increases in parallel with the increased production of these cytokines.

MD-1 protein increase in supernatant of BMDM

We considered what kinds of cells express and secrete soluble MD-1 during inflammatory response. Sasaki *et al*. showed that 24–72 h cultured BMDM secreted sMD-1 by using a binding assay to the RP105 alone-expressing Ba/F3 cells (13). We analyzed whether TLR ligands increase the levels of MD-1 protein in supernatant of BMDM or not. As shown in Fig. 4(A), the levels of MD-1 protein increased in 48-h Lipid A or DH5α stimulated supernatant compared with non-stimulated supernatant. To show the reproducibility, we tried the same experiments of Fig. 4(A) by using four different mice. As shown in Fig. 4(B), we could show a 1.5 times increase in Lipid A or DH5α stimulated samples compared with non-stimulated samples.

These results show that macrophages are one of the candidates of MD-1-producing cells during inflammatory responses.

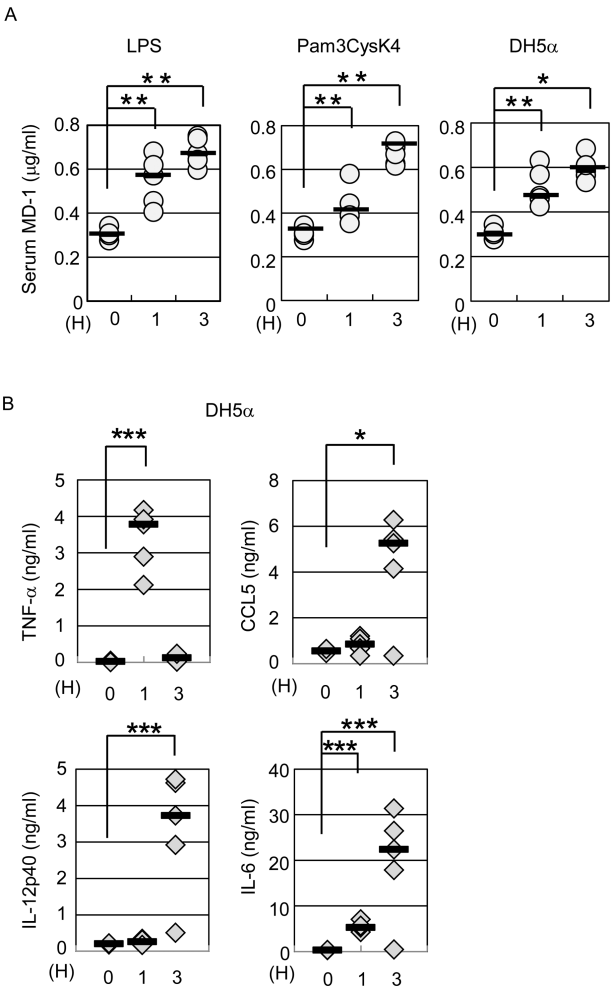

Fig. 3. Serum MD-1 increases in case of infection. (A) Twelve-week C57BL/6 ($n = 4$ or 5) female mice were administered with LPS (2.5 μg/mouse, 125 μg/kg), Pam3CysK4 (100 μg/mouse, 5 mg/kg) or heat-killed DH5α (3.5×10^9/ml CFU) intraperitoneally. Blood samples were collected from vena cava at 0 (no treatment), 1 and 3 h after injection. The concentration of MD-1 was determined by ELISA. (B) The concentrations of TNF-α, IL-6, IL-12p40 and CCL5 of DH5α injected blood samples from (A) were determined by ELISA. Data represent the SD. Horizontal bars denote mean values. $^*P < 0.05$, $^{**}P < 0.01$, $^{***}P < 0.005$.

MD-1 concentration is affected by diet and ischemia/reperfusion injury

We focused on the increased levels of serum MD-1. We studied MD-1 concentrations under several conditions, and we found that the HiFat/HiSucrose diet causes an increased serum MD-1 (Fig. 5A). Surprisingly, MD-1 was also found in urine, and the concentration (μg/ml per urine creatinine) on day 1 was also increased (Fig. 5A). It was immediately apparent from these data that the HiFat and HiSucrose diet induced MD-1 production.

Next, we analyzed serum or plasma MD-1 concentration in renal or liver I/R injury. In the reperfusion state, various kinds of toxic materials, for example, reactive oxygen species, nitric oxide, many kinds of chemical mediator are produced. Then, they induce neutrophil activation and blood vessel

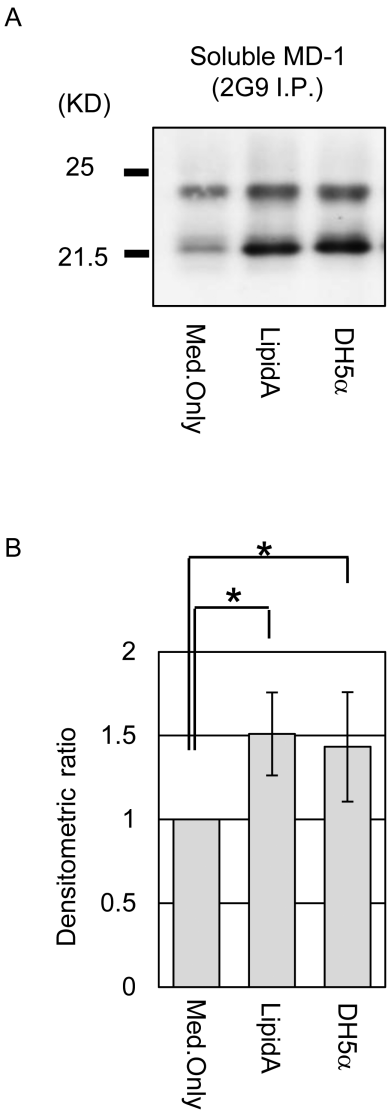

Fig. 4. The expression of MD-1 increases in the supernatant of BMDM by pathogen ingredient stimulation. (A) BMDM were prepared from four different 16- to 20-week C57BL/6 female mice. BMDM were placed in a six-well plate (2×10^6/well/2 ml) and incubated with or without Lipid A (2 μg/ml) or DH5α (5×10^6/ml CFU) for 48 h. After incubation, the supernatants were collected and immunoprecipitated with anti-MD-1 mAb (JR2G9). The precipitates were probed with anti-MD-1 polyclonal Ab, followed by biotinylated goat anti-rabbit Ig as a secondary antibody, finally followed by streptavidin-horseradish peroxidase conjugated antibody. (B) Densitometric scanning of the MD-1 bands was used for estimation of ratio. A densitometric volume of the I.P. sample from the medium only in each experiment is set to 1. Data obtained from samples of four independent mice are shown. Data are presented as the mean ± SD values derived from four different experiments $^*P < 0.05$.

endothelium injury, microcirculation disorder and finally organ failure (23). Compared with the sham samples, the serum MD-1 concentration from renal reperfusion samples was elevated (Fig. 5B). Plasma MD-1 is also increased in liver reperfusion injury (Fig. 5B). To elevate serum MD-1 concentration an ischemic time of >90 min is needed. These results suggest that the I/R injury induces MD-1 production. From these results, the MD-1 concentration is influenced by infection, diet and I/R injury. A fixed quantity of MD-1 always exists in serum and urine, and the quantity of production is immediately influenced by infection, diet and ischemic situations.

Discussion

The newly established mAbs are useful for multiple assays. JR7G1 is able to detect not only MD-1 associated with RP105 but also MD-1 alone. JR7G1 is useful for FACS and immunoprecipitation assay. JR2G9 is able to detect the MD-1 alone, and the epitope is considered close to the RP105-binding site. In the MD-1 ELISA, JR7G1 is used as a capture antibody, and JR2G9 is used as a detection antibody. In a past report, rat hybridoma (SH1.2.47) was the first report about an anti-MD-1 mAb (24). The report showed cell-surface MD-1 expression by FACS and IP assay; however, soluble MD-1 was not mentioned. Before we reported the anti-MD-1 mAb, MD14, which was able to detect only the RP105-associated MD-1 (3) and MD14 is not able to be used in IP assay (Supplementary Fig. S1C, available at *International Immunology* Online). On the other hand, JR7G1 is useful for every assay. JR7G1 is a slightly agonistic antibody and elicits proliferation of spleen cells (Fig. 2B). In the dexamethasone-induced apoptotic assay, JR7G1 slightly suppressed apoptosis (Fig. 2A). JR7G1 accelerates TLR stimulation on spleen cells but competitively inhibits anti-RP105 or anti-IgM mAb-induced proliferation. Anti-RP105 mAb induces a competitive signal against anti-IgM stimulation (25, 26). It is predicted that JR7G1 changes the conformation of the RP105/MD-1 complex, suppressing the aggregation of RP105/MD-1 molecules and inhibiting the proliferation of spleen cells by anti-RP105 mAb. JR7G1 partially inhibited anti-IgM mAb stimulation. The mechanism is unknown, and we are now analyzing the relationship between MD-1 and the B-cell receptor.

This study has determined the MD-1 concentration in serum. In B6 wild-type mice, 0.29–0.91 μg/ml of MD-1 was detected in serum. The concentration was increased a little with age (Supplementary Fig. S2, available at *International Immunology* Online). The MD-1 concentration of serum from $RP105^{-/-}$ mice was slightly higher than wild-type mice. There is a possibility that MD-1 binds to the cell-surface RP105 and regulates the free-soluble concentration of MD-1. We found that MD-1 rapidly increased in serum after the injection of TLR ligands (Fig. 3A). As shown in Fig. 3A, the serum MD-1 rapidly increased like C-reactive protein (CRP). There are several common characteristics with MD-1 and CRP. For example, both have a phospholipid-binding site and are secreted from macrophages (27). The high-fat diet (HFD), ischemic state or the elevation of autoimmune activity also induces production in serum (28). However, we could not find a report about the rapid elevation of CRP by pathogen component injection as shown in MD-1 (Fig. 3A). MD-1 will be a more sensitive inflammatory biomarker than CRP.

As mentioned above, after TLR ligand injection, serum MD-1 increased rapidly. However, we could not detect the increase of MD-1 concentration in supernatant of BMDM by TLR ligand stimulation after 1–3 h. As shown in Fig. 4(A and B), we could show a little increase of MD-1 in supernatant of BMDM after 48-h TLR ligand stimulation. We cannot explain

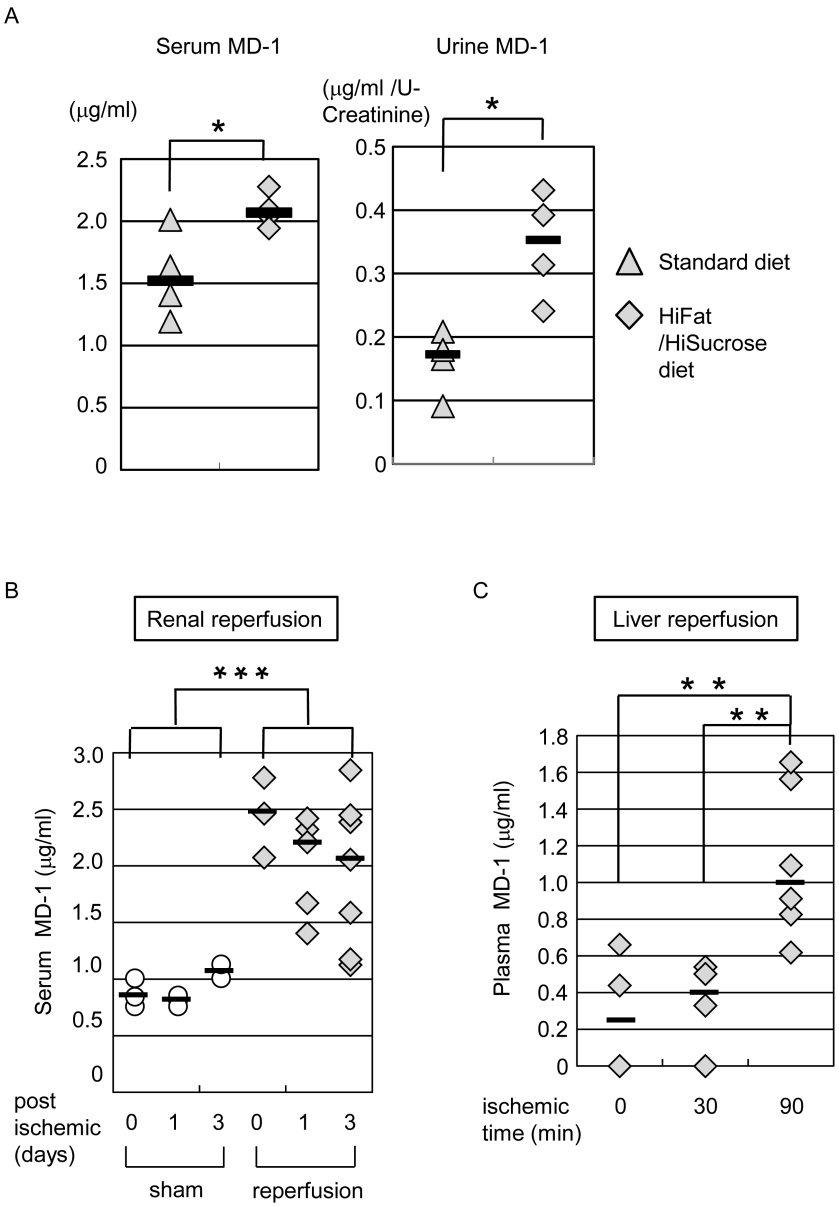

Fig. 5. Serum and urine MD-1 increase in HiFat/HiSucrose diet and reperfusion injury. (A) C57BL/6 (n = 4) mice were bred under a HiFat/HiSucrose diet as described in Materials and Methods. Blood samples were collected from vena cava. The concentration of MD-1 was determined by ELISA. (B) Renal reperfusion was initiated as described in Materials and Methods. Blood samples of sham (Day 0: n = 3, Day 1: n = 3, Day 3: n = 2) or reperfusion (Day 0: n = 3, Day 1: n = 5, Day 3: n = 7) mice were collected and the concentration of MD-1 determined by ELISA.. (C) Liver reperfusion injury was administrated as described in Materials and Methods. Liver reperfusion was initiated after 0 (n = 4), 30 (n = 4) or 90 min (n = 6) of ischemia by removal of the clamp. After 6 or 24 h of reperfusion, blood samples were collected from the inferior vena cava and the concentration of MD-1 determined by ELISA. Horizontal bars denote mean values. $^{**}P < 0.01$, $^{***}P < 0.005$.

the reason why the necessary time for the increase of MD-1 in serum and on a macrophage is so different. Sometimes the discrepancy is recognized in cytokine production. For example, Gozzi *et al*. reported that the peak time of TNF-α production in mice serum was 1.5 h after LPS injection (29), but Hagiwara *et al*. reported that in supernatants from mouse macrophages, the peak time was 24 h after LPS stimulation (30). In any case, we could show the MD-1 expression in supernatant of BMDM by anti-MD-1 mAb IP assay. From these results, it is probable that macrophages are only one of the candidates of MD-1-producing cells.

Watanabe *et al*. demonstrated that the RP105/MD-1 complex contributed to HFD-induced obesity, adipose tissue inflammation and insulin resistance (31). RP105$^{-/-}$ and MD-1$^{-/-}$ mice had less HFD-induced adipose tissue inflammation, hepatic steatosis and insulin resistance compared with wild-type and TLR4$^{-/-}$ mice. Because MD-1 has a low-specific phospholipid-binding pockets (32), it may function as a lipid transfer protein in serum. One of the lipid transporters, PLTP, mediates transfer of phospholipids from apoB-containing triglyceride-rich lipoprotein into High-density lipoprotein and exchanges phospholipids between

lipoproteins (33). Several articles showed that PLTP associates with the onset of obesity and arteriosclerosis (33, 34). Karper *et al*. demonstrated that RP105 also influences atherosclerotic plaque formation by using RP105$^{-/-}$ chimera mice (35). MD-1 may work as a PLTP, and the RP105/MD-1-induced signal may be important for induction of the tissue inflammation, obesity and atherosclerosis.

Our results show that infection, HFD and reperfusion injury induce MD-1 production in serum and urine. It is well known that these are endoplasmic reticulum (ER) stress triggers (36). ER stress participates in the onset and progress of disease such as diabetes, neurodegenerative diseases including Parkinson's disease, heart problems and atherosclerosis. A recent report shows that ER stress activates the inflammasome via NLRP3- and Caspase-2-driven mitochondrial damage under inflammatory responses on macrophages (37). Our result shows that macrophages express soluble MD-1 protein and it increases in the inflammatory state. MD-1 may work as a sensor of ER stress.

Koarada *et al*. showed that the number of RP105-negative B cells increases in the case of B-cell-activated disease, such as systemic lupus erythematosus, dermatomyositis and Sjögren's syndrome. They showed that the number of RP105-negative B cells decreases after therapy; therefore, they are insisting that the negative RP105 is an activity marker of autoimmune disease (15, 16). There is a possibility that MD-1 is actively released during the highly active state of autoimmune disease, through the internalization of RP105, and increases the number of RP105-negative B cells. Anti-human MD-1 mAb is needed for further analysis of the function and concentration of human MD-1 in serum.

In conclusion, the present study identified the concentration of serum and urine MD-1 by establishment of two kinds of anti-MD-1 mAbs. MD-1 increases in ER stress such as infection, HFD and reperfusion injury. There is a possibility that macrophage secretes MD-1 in situations such as ER stress. Establishment of human MD-1 ELISA system will be needed as an easy and sharp detection method of ER stress.

Supplementary data

Supplementary data are available at *International Immunology* Online.

Funding

Grants-in-Aid for Scientific Research (C) from the Ministry of Education, Culture, Sports, Science and Technology of the Japanese Government (23590564 and 15K09491); a Grant for the Joint Research Project of the Institute of Medical Science, the University of Tokyo (I.D. No. 340 and I.D. No. 356); a Grant from the Aichi Cancer Research Foundation; a Grant from the Okinaka Memorial Institute for Medical Research; and a Grant from the AiKei-Kai Foundation.

Acknowledgements

The authors have no conflicting financial interests. We thank N. Tanimura and Y. Motoi for excellent technical assistance and helpful discussions.

References

1 Chen, G. Y. and Nuñez, G. 2010. Sterile inflammation: sensing and reacting to damage. *Nat. Rev. Immunol.* 10:826.
2 Miyake, K., Shimazu, R., Kondo, J. *et al.* 1998. Mouse MD-1, a molecule that is physically associated with RP105 and positively regulates its expression. *J. Immunol.* 161:1348.
3 Nagai, Y., Shimazu, R., Ogata, H. *et al.* 2002. Requirement for MD-1 in cell surface expression of RP105/CD180 and B-cell responsiveness to lipopolysaccharide. *Blood* 99:1699.
4 Miura, Y., Shimazu, R., Miyake, K. *et al.* 1998. RP105 is associated with MD-1 and transmits an activation signal in human B cells. *Blood* 92:2815.
5 Miyake, K., Yamashita, Y., Ogata, M., Sudo, T. and Kimoto, M. 1995. RP105, a novel B cell surface molecule implicated in B cell activation, is a member of the leucine-rich repeat protein family. *J. Immunol.* 154:3333.
6 Liu, Y., Yin, H., Zhao, M. and Lu, Q. 2014. TLR2 and TLR4 in autoimmune diseases: a comprehensive review. *Clin. Rev. Allergy Immunol.* 47:136.
7 Nagai, Y., Kobayashi, T., Motoi, Y. *et al.* 2005. The radioprotective 105/MD-1 complex links TLR2 and TLR4/MD-2 in antibody response to microbial membranes. *J. Immunol.* 174:7043.
8 Kimoto, M., Nagasawa, K. and Miyake, K. 2003. Role of TLR4/MD-2 and RP105/MD-1 in innate recognition of lipopolysaccharide. *Scand. J. Infect. Dis.* 35:568.
9 Liu, B., Zhang, N., Liu, Z. *et al.* 2013. RP105 involved in activation of mouse macrophages via TLR2 and TLR4 signaling. *Mol. Cell. Biochem.* 378:183.
10 Blumenthal, A., Kobayashi, T., Pierini, L. M. *et al.* 2009. RP105 facilitates macrophage activation by *Mycobacterium tuberculosis* lipoproteins. *Cell Host Microbe* 5:35.
11 Kobayashi, T., Takahashi, K., Nagai, Y. *et al.* 2008. Tonic B cell activation by radioprotective 105/MD-1 promotes disease progression in MRL/lpr mice. *Int. Immunol.* 20:881.
12 Pugin, J., Stern-Voeffray, S., Daubeuf, B., Matthay, M. A., Elson, G. and Dunn-Siegrist, I. 2004. Soluble MD-2 activity in plasma from patients with severe sepsis and septic shock. *Blood* 104:4071.
13 Sasaki, S., Nagai, Y., Yanagibashi, T. *et al.* 2012. Serum soluble MD-1 levels increase with disease progression in autoimmune prone MRL(lpr/lpr) mice. *Mol. Immunol.* 49:611.
14 Ohto, U., Miyake, K. and Shimizu, T. 2011. Crystal structures of mouse and human RP105/MD-1 complexes reveal unique dimer organization of the toll-like receptor family. *J. Mol. Biol.* 413:815.
15 Koarada, S., Tada, Y., Suematsu, R. *et al.* 2012. Phenotyping of P105-negative B cell subsets in patients with systemic lupus erythematosus. *Clin. Dev. Immunol.* 2012:198206.
16 Koarada, S., Tashiro, S., Nagao, N., Suematsu, R., Ohta, A. and Tada, Y. 2013. Increased RP105-negative B cells in IgG4-related disease. *Open Rheumatol. J.* 7:55.
17 Shimazu, R., Akashi, S., Ogata, H. *et al.* 1999. MD-2, a molecule that confers lipopolysaccharide responsiveness on Toll-like receptor 4. *J. Exp. Med.* 189:1777.
18 Ogata, H., Su, I., Miyake, K. *et al.* 2000. The Toll-like receptor protein RP105 regulates lipopolysaccharide signaling in B cells. *J. Exp. Med.* 192:23.
19 Mori, K., Lee, H. T., Rapoport, D. *et al.* 2005. Endocytic delivery of lipocalin-siderophore-iron complex rescues the kidney from ischemia-reperfusion injury. *J. Clin. Invest.* 115:610.
20 Haga, S., Remington, S. J., Morita, N., Terui, K. and Ozaki, M. 2009. Hepatic ischemia induced immediate oxidative stress after reperfusion and determined the severity of the reperfusion-induced damage. *Antioxid. Redox Signal.* 11:2563.
21 Ozaki, M., Suzuki, S. and Irani, K. 2002. Redox factor-1/APE suppresses oxidative stress by inhibiting the rac1 GTPase. *FASEB J.* 16:889.
22 Miyake, K., Yamashita, Y., Hitoshi, Y., Takatsu, K. and Kimoto, M. 1994. Murine B cell proliferation and protection from apoptosis with an antibody against a 105-kD molecule: unresponsiveness of X-linked immunodeficient B cells. *J. Exp. Med.* 180:1217.
23 McCord, J. M. 1985. Oxygen-derived free radicals in postischemic tissue injury. *N. Engl. J. Med.* 312:159.

24 Hadidi, S., Yu, K., Chen, Z. and Gorczynski, R. M. 2001. Preparation and functional properties of polyclonal and monoclonal antibodies to murine MD-1. *Immunol. Lett.* 77:97.
25 Yamashita, Y., Miyake, K., Miura, Y. *et al.* 1996. Activation mediated by RP105 but not CD40 makes normal B cells susceptible to anti-IgM-induced apoptosis: a role for Fc receptor coligation. *J. Exp. Med.* 184:113.
26 Chan, V. W., Mecklenbräuker, I., Su, I. *et al.* 1998. The molecular mechanism of B cell activation by toll-like receptor protein RP-105. *J. Exp. Med.* 188:93.
27 Ciubotaru, I., Potempa, L. A. and Wander, R. C. 2005. Production of modified C-reactive protein in U937-derived macrophages. *Exp. Biol. Med. (Maywood)* 230:762.
28 Thiele, J. R., Zeller, J., Bannasch, H., Stark, G. B., Peter, K. and Eisenhardt, S. U. 2015. Targeting C-reactive protein in inflammatory disease by preventing conformational changes. *Mediators Inflamm.* 2015:372432.
29 Gozzi, P., Påhlman, I., Palmér, L., Grönberg, A. and Persson, S. 1999. Pharmacokinetic-pharmacodynamic modeling of the immunomodulating agent susalimod and experimentally induced tumor necrosis factor-alpha levels in the mouse. *J. Pharmacol. Exp. Ther.* 291:199.
30 Hagiwara, S., Iwasaka, H., Hidaka, S., Hishiyama, S. and Noguchi, T. 2008. Danaparoid sodium inhibits systemic inflammation and prevents endotoxin-induced acute lung injury in rats. *Crit. Care* 12:R43.
31 Watanabe, Y., Nakamura, T., Ishikawa, S. *et al.* 2012. The radioprotective 105/MD-1 complex contributes to diet-induced obesity and adipose tissue inflammation. *Diabetes* 61:1199.
32 Harada, H., Ohto, U. and Satow, Y. 2010. Crystal structure of mouse MD-1 with endogenous phospholipid bound in its cavity. *J. Mol. Biol.* 400:838.
33 Jiang, X. C., Jin, W. and Hussain, M. M. 2012. The impact of phospholipid transfer protein (PLTP) on lipoprotein metabolism. *Nutr. Metab. (Lond)* 9:75.
34 Tzotzas, T., Desrumaux, C. and Lagrost, L. 2009. Plasma phospholipid transfer protein (PLTP): review of an emerging cardiometabolic risk factor. *Obes. Rev.* 10:403.
35 Karper, J. C., de Jager, S. C., Ewing, M. M. *et al.* 2013. An unexpected intriguing effect of Toll-like receptor regulator RP105 (CD180) on atherosclerosis formation with alterations on B-cell activation. *Arterioscler. Thromb. Vasc. Biol.* 33:2810.
36 Kim, I., Xu, W. and Reed, J. C. 2008. Cell death and endoplasmic reticulum stress: disease relevance and therapeutic opportunities. *Nat. Rev. Drug Discov.* 7:1013.
37 Bronner, D. N., Abuaita, B. H., Chen, X. *et al.* 2015. Endoplasmic reticulum stress activates the inflammasome via NLRP3- and caspase-2-driven mitochondrial damage. *Immunity* 43:451.